

Journal of Mechanics of Materials and Structures

**EFFECTS OF CONTACT SURFACE SHAPE ON LIFETIME OF CELLULAR
FOCAL ADHESION**

Gregory J. Rizza, Jin Qian and Huajian Gao

Volume 6, No. 1-4

January–June 2011

EFFECTS OF CONTACT SURFACE SHAPE ON LIFETIME OF CELLULAR FOCAL ADHESION

GREGORY J. RIZZA, JIN QIAN AND HUAJIAN GAO

As a means of better understanding cell-matrix adhesion, we consider the effects that the contact surface shape of a cellular focal adhesion has on its adhesion lifetime. An idealized model of focal adhesion is adopted in which two dissimilar elastic media are bonded together by an array of ligand/receptor bonds modeled as Hookean springs on a curved surface. The cluster of bonds is subjected to a constant applied tensile load F , and the distribution of traction forces on the individual bonds is assumed to obey the elasticity equations of continuous elastic media. The rupturing and rebinding of bonds are described by stochastic equations solved using the Monte Carlo method. The contact surface in the model is scaled by an optimal shape defined as the deformed surface profile of a planar elastic half-space that is subjected to a uniform pressure applied over the contact region with the total force equal to F . Our model shows that contact surface shape does have a substantial impact on adhesion lifetime. The model also shows that the adhesion lifetime becomes increasingly sensitive to variations in contact surface shape as the focal adhesion increases in size.

1. Introduction

Cell adhesion is becoming an important topic of study in all fields involving cellular research. It has been observed that a large amount of cell activities such as cell migration, cell differentiation, wound healing, etc. are dependent upon the ability of a cell to adhere to a variety of biological surfaces [Alberts et al. 2002; Chen and Gumbiner 2006]. An interesting feature of cell adhesion on substrates, which could be characterized as a cell adhering to the extracellular matrix (ECM) within an organism of study, is that the bonds formed between the cell surface and ECM via ligand/receptor connections are usually arranged in clusters of multiple individual bonds [Zamir et al. 2000; Zaidel-Bar et al. 2003]. These bond clusters are of a finite size with a maximum length of only a few microns depending on the stiffness of the system, and have been referred to as focal adhesions (FAs) due to their definite size and discreteness [Alberts et al. 2002; Chen and Gumbiner 2006; Zamir et al. 2000; Zaidel-Bar et al. 2003; Bershadsky et al. 2003]. There are many biological, chemical and mechanical processes which occur during the sequences involved in cellular adhesion. However, for the purposes of this paper we will only examine cellular focal adhesion on the basis of a mechanical model in order to develop a better understanding of the effects of contact surface shape on FA lifetime.

There have been both theoretical and experimental studies in developing an understanding that single ligand/receptor bonds only have finite adhesion lifetime. Even in the absence of any applied load, bond dissociations due to thermal fluctuation are expected to occur in a statistical fashion [Evans and Ritchie

Keywords: cell adhesion, focal adhesion, ligand/receptor bonds, optimal shape, adhesion lifetime, Monte Carlo method, biomechanics.

1997; Evans 2001; Evans and Calderwood 2007]. This understanding of single molecular bonds is currently accepted and assumed to be representative of the behavior of a large number of ligand/receptor types in cell adhesion. However, the mechanics of multiple bond adhesions, such as those in focal adhesions, is not understood to the same degree of single bond adhesion due to its complexity.

The study of adhesions made up of many molecular bonds was pioneered by Bell [1978], who developed a kinetic theory to predict the thermodynamic competition between bonds forming and breaking under an applied load. The investigation of multiple bond adhesion was further progressed by the work of Erdmann and Schwartz [2004a; 2004b] who developed stochastic equations and performed Monte Carlo simulations to investigate the adhesion lifetime as a function of cluster size. They showed that, unlike single bond adhesion which only has a limited lifetime, focal adhesion clusters made up of multiple bonds could have more prolonged lifetimes. Their model showed that the larger the focal adhesion becomes the longer adhesion lifetime it can experience. Qian et al. [2008; 2009] were the first to model focal adhesions between cell and substrate in terms of clusters of ligand/receptor bonds between two dissimilar continuous elastic media, showing the effects of varying adhesion size and system stiffness on focal adhesion strength and lifetime. According to their results, a possible explanation for the characteristic micron-size scale of focal adhesions is that small adhesion size leads to single-molecule-like behavior of limited lifetime because of statistical effects whereas large adhesion also leads to single-molecule-like behavior because of the focusing effect of stress concentration that confines the bond dissociation events to a smaller number of bonds near the adhesion edges. Their model also showed that stiffer cell and substrate result in larger and more stable focal adhesions than softer ones. This finding is consistent with a range of experimental observations, including that focal adhesions are small or absent in cells cultured on sufficiently compliant substrates, and that cells tend to actively migrate towards stiffer region when cultured on an elastically nonhomogeneous substrate [Pelham and Wang 1997; Lo et al. 2000; Tan et al. 2003].

So far we know that clustering multiple bonds into focal contacts greatly enhances the lifetime and stability of cell-matrix adhesion [Erdmann and Schwarz 2004a; 2004b]. However, due to the elasticity effects of the system, there is an upper limit in size of a focal adhesion in order for it to avoid stress concentration effect [Qian et al. 2008; 2009]. It has also been shown that stiffness of cell and substrate is a factor in controlling the stability of focal adhesions, and cells have a preference towards stiffer substrates potentially due to the increased focal adhesion lifetime [Qian et al. 2008; 2009].

The present paper explores how contact surface shape can be used as a factor to control focal adhesion lifetime. Here, the contact surface shape is defined as the initial gap between a pair of contacting surfaces in the absence of any external loads [Gao and Yao 2004; Yao and Gao 2006]. In the special case when one of the contact surfaces is a flat plane, the contact surface shape then corresponds to the actual shape of the opposing partner surface. Optimization of contact surface shape is not an uncommon strategy when trying to increase adhesion strength in contact mechanics problems. In biology, optimized surface shapes can be seen in species that rely on nonspecific adhesion for survival such as gecko and many types of insects, and the optimal surface shape for adhesion between two elastic media via van der Waals interaction has been defined as the profile of the contact surface that distributes an applied load uniformly within the adhesion region at the critical moment of pull-off [Gao and Yao 2004; Yao and Gao 2006; Shi et al. 2006]. Following a similar line of thought, here we define the optimal contact surface shape of focal adhesions via specific molecular bonds as the shape that gives rise to a uniform traction distribution

among individual bonds within the adhesion domain whenever the closed bonds are evenly spaced. This even distribution of load avoids stress concentrations along the contact edges, leading to substantially increased lifetime of focal adhesions.

The goal of this article is to explore the effects of contact surface shape on focal adhesion lifetime. Based on previous studies on the lifetime of multiple bond adhesion under constant tensile loads, we plan to demonstrate the effects that altering and optimizing the geometric shape of the adhesion surface have on focal adhesion lifetime. To do this, a range of surface shapes which are related to the optimal shape through a numerical shape factor are studied under various focal adhesion parameters. From this model, we plan to show:

- (1) Optimizing surface shape can greatly increase focal adhesion lifetime.
- (2) As focal adhesions increase in size, deviations from the optimal shape result in substantial decrease in adhesion lifetime when compared to the cases of focal adhesions with fewer bonds.
- (3) Varying system stiffness and applied tensile load on the focal adhesion have interesting effects with respects to parts (1) and (2).

2. Model

The theoretical model under consideration is illustrated in Figure 1, in which two elastic media are seen bonding to each other via ligand/receptor bonds. The upper elastic medium represents a biological cell whereas the lower elastic medium is representative of the extracellular matrix. The Young's moduli and

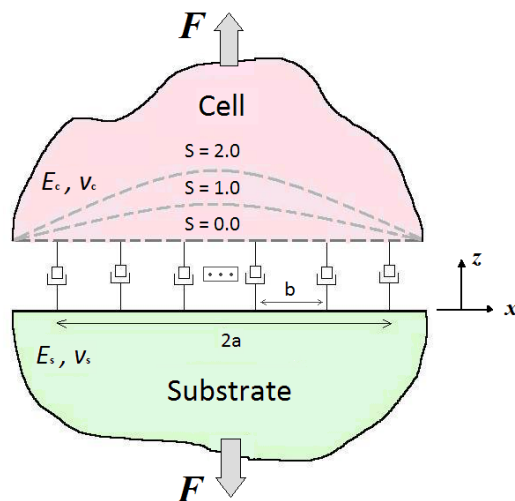


Figure 1. Idealized model of a single focal adhesion between a cell and substrate undergoing tensile loading. The cell and substrate are bonded together by an array of ligand/receptor bonds. The contact surface shapes of the focal adhesion are determined by a shape factor S which ranges in $[0, 2]$, where $S = 1$ corresponds to the optimal contact shape for an initial uniformly loaded bond cluster.

Poisson’s ratios of these media are defined as E_c, ν_c for the cell, and E_s, ν_s for the substrate. It is usually convenient to define a combined elastic modulus E^* as

$$\frac{1}{E^*} = \frac{1 - \nu_c^2}{E_c} + \frac{1 - \nu_s^2}{E_s} \tag{2-1}$$

when analyzing contact problems involving two different elastic media [Johnson 1985]. The cell/substrate system is subject to a constant tensile load F such that the load distribution among individual bonds is governed by elasticity equations. The two media are bonded together by ligand/receptor bonds idealized as Hookean springs with a spring coefficient k_{LR} . It is assumed in the model that the bonds do not have any interaction with each other. It is also assumed that when rupture occurs in a bond, the energy required to rupture the ligand/receptor bond is much lower than the energy required to rupture the connection of the ligand or receptor from the cell or substrate surface [Bell 1978]. What this means is when the ligand/receptor bond is undergoing tensile loading, rupturing of the bond will most likely occur at the ligand/receptor interface due to the less energy required for it to rupture. The bonds are evenly spaced at distance b from each other in the lateral x -direction (Figure 1), corresponding to a bond density of $\rho_{LR} = 1/b^2$. As can be seen in Figure 2, the initial location of each bond in the vertical z -direction is determined by a shape factor S . The shape factor value of $S = 0$ corresponds to the surfaces of the cell and substrate being modeled as horizontal planes, $S = 1$ corresponds to an optimized curved surface profile that gives rise to uniform traction distribution among individual ligand/receptor bonds within the adhesion domain under a tensile load (see details in next section), and $S = 2$ corresponds to an overly curved surface in comparison to the optimal surface ($S = 1$). The adhesion being analyzed in this model is defined as a single focal adhesion cluster which is made up of an array of bonds aligned axially with

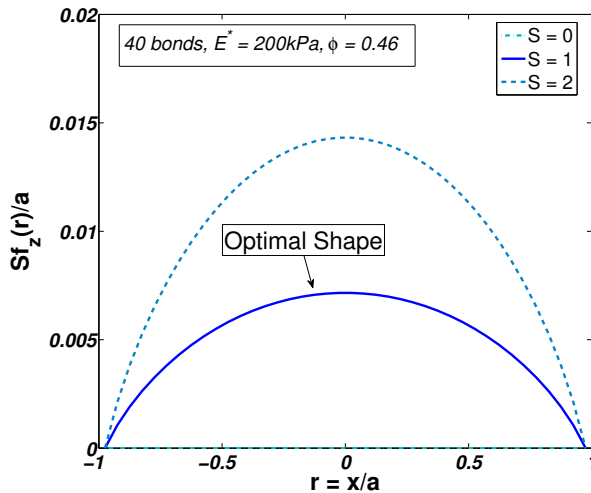


Figure 2. Schematic of a focal adhesion surface containing 40 bonds, having a system stiffness of $E^* = 200$ kPa, and a tensile load factor of $\varphi = 0.46$. The surface shapes represented are for the following shape factors: $S = 0$ corresponding to adhesion between conforming surfaces, $S = 1$ corresponding to the optimal shape, and $S = 2$ corresponding to an overly curved focal adhesion surface in comparison to the optimal case.

an out of plane thickness b . The size of the adhesion is defined as $2a$ where a is the half-width of the focal adhesion, and the total number of involved bonds is $N = 2a/b$.

2.1. Optimal shape and shape factor. Following a similar concept introduced in reference [Gao and Yao 2004], an optimal shape of contact surface is defined as the deformed surface profile of a planar half-space that is subjected to a uniform pressure applied over the contact region with the total force equal to F on the bond cluster. For a cluster of evenly spaced ligand/receptor bonds, the optimal contact surface shape that gives rise to a uniform traction distribution among individual bonds within the adhesion domain is

$$f_z(x) = -\frac{\varphi \cdot F_b}{\pi E^* b^2} \left((a+x) \ln \left(\frac{a+x}{a} \right)^2 + (a-x) \ln \left(\frac{a-x}{a} \right)^2 + C_x \right), \quad (2-2)$$

where C_x is a length constant to satisfy the condition that the optimal shape gives $z = 0$ at a reference point x_∞ , F_b is a force scale related to the dissociation of single bonds (see (2-9) below), and $\varphi = F/(F_b N)$ is a load factor representing the nominal force sustained by individual bonds (normalized by the force scale F_b).

As can be seen in Figure 2, a shape factor S has been applied to the elasticity part of modeling in order to study the effects of surface shape on adhesion lifetime. The shape factor S is defined in such a way that $S = 0$ corresponds to two bonded surfaces in perfect conformity with each other in the absence of external loads, $S = 1$ corresponds to the optimal contact surface shape defined in (2-2), and $S = 2$ corresponds to an overly curved surface when compared to the optimal surface shape.

2.2. Elasticity model. Let us define the axial direction running parallel to the surfaces of the cell and substrate to be x , and assume that the origin $x = 0$ corresponds to the center of the focal adhesion. Also, let us define $u(x)$ to be the difference between the stretched length of the ligand/receptor bond located at position x and its rest length l_b , and $w(x)$ be the surface displacement discontinuity of the two elastic media at x . The relationship between $u(x)$ and $w(x)$ is governed by the compatibility condition at the cell-substrate interface, to ensure that the bond length after deformation, $u(x) + l_b$, is equal to the displacement and shape discontinuities, $-w(x)$ and $S \cdot f_z(x)$, plus a constant separation h , i.e.,

$$u(x) + w(x) + l_b = h + S \cdot f_z(x). \quad (2-3)$$

In our model, x_i is constricted to the domain of $[-a, a]$ and is representative of the location of a bond in the x direction within a focal adhesion of size $2a$. The elastic Green's function that defines the relative displacement of the combined elastic media at position x_i induced by a load being applied on a bond at x_j ($i \neq j$) is given by the equation [Johnson 1985]

$$w_{ij} = \frac{1}{\pi E^* b} \cdot 2F_j (\ln |x_\infty - x_j| - \ln |x_i - x_j|), \quad (2-4)$$

where F_j is the individual force acting on the bond at location x_j , and x_∞ is an arbitrary reference point chosen such that $w_{ij} = 0$ at x_∞ for a load F_j . To avoid singularity, the relative displacement of the elastic media at position x_i caused by the on-site load F_i acting on the bond is given by the equation [Johnson 1985]

$$w_{ii} = -\frac{1}{\pi E^*} \cdot \frac{F_i}{2a_0 b} (2a_0 \ln 4 + C_i), \quad (2-5)$$

where a_0 denotes the radius of an individual bond and is typically only a few nanometers [Arnold et al. 2004], and C_i is a length constant chosen such that $w_{ii} = 0$ at x_∞ .

Since we have chosen to model ligand/receptor bonds as Hookean springs, the relationship between the extension of a bond at a position x_i and the load F_i applied on that bond is

$$F_i = k_{\text{LR}} u_i. \quad (2-6)$$

Combining Equations (2-3)–(2-6) gives the elasticity equation

$$\sum_{j=1, j \neq i}^n \left\{ \frac{1}{\pi E^* b} 2F_j (\ln |x_\infty - x_j| - \ln |x_i - x_j|) \right\} - \frac{1}{\pi E^*} * \frac{F_i}{2a_0 b} (2a_0 \ln 4 + C_i) + \frac{F_i}{k_{\text{LR}}} + l_b = h + S \cdot f_z(x_i), \quad (2-7)$$

where n is the number of closed bonds in the focal adhesion. This relationship in (2-7) represents n equations with $n + 1$ unknowns (F_1, \dots, F_n, h). The elastic part of the model is completed with an additional equation coming from the global force balance

$$\sum_{i=1}^n F_i = F = \varphi F_b N, \quad (2-8)$$

where F is the constant tensile load being applied to the system.

2.3. Stochastic model. The elasticity equations shown above govern how the applied load F is distributed among all closed bonds. Each bond site within the focal adhesion in the present model has the ability to rupture from attachment as well as rebind after rupture. These rupturing and rebinding behaviors are represented as rate equations and are defined using the following stochastic equations.

Bond rupturing is assumed to occur according to [Bell 1978]

$$k_{\text{off}} = k_0 e^{F_i/F_b}, \quad (2-9)$$

where the rate of bond rupture increases exponentially as the load acting on the individual bonds F_i increases. The rate of bond rupture as defined by Bell involves the parameters F_b , which is a force scale typically in the piconewton range [Bell 1978], and k_0 , which is the spontaneous dissociation rate of an individual bond in the absence of any type of load. The spontaneous dissociation rate can range anywhere from 0.1 to 100 seconds depending on the bond type and environmental conditions [Evans and Calderwood 2007].

Bond rebinding behavior is assumed to depend on the separation distance between the open receptor and free hanging ligand as described by Erdmann and Schwarz [2007; 2006], which the reader can consult for the next few equations. The probability of a ligand falling in close proximity to a receptor within a reacting radius l_{bind} is

$$p = \frac{l_{\text{bind}}}{Z} e^{-k_{\text{LR}}(\delta - l_b)^2 / (2k_B T)}, \quad (2-10)$$

where l_{bind} is defined as the length scale within which the receptor and ligand will react to form a bond, δ is the surface separation between cell and substrate where the open receptor and ligand are anchored,

$k_B T$ is the Boltzmann constant multiplied by the absolute temperature, and Z is a partition function defined as

$$Z = \sqrt{\frac{\pi k_B T}{2k_{LR}}} \left\{ \operatorname{erf} \left((\delta - l_b) \sqrt{\frac{k_{LR}}{2k_B T}} \right) + \operatorname{erf} \left(l_b \sqrt{\frac{k_{LR}}{2k_B T}} \right) \right\}. \quad (2-11)$$

From these equations, the rebinding rate can be defined as

$$k_{\text{on}} = k_{\text{on}}^0 \frac{l_{\text{bind}}}{Z} e^{-k_{LR}(\delta - l_b)^2 / (2k_B T)}, \quad (2-12)$$

where k_{on}^0 is a spontaneous reaction rate of open ligand/receptor pairs within the reacting radius l_{bind} . It is beneficial to normalize both the rupture and rebinding rates in our model in order to define certain analytical factors. Both the rupture and rebinding rates are defined by

$$r_i = e^{F_i / F_b}, \quad (2-13)$$

$$g_i = 2\gamma \sqrt{\frac{\beta}{\pi}} \frac{e^{-\beta(\Delta_i - L_b)^2}}{\operatorname{erf}(\sqrt{\beta}(\Delta_i - L_b)) + \operatorname{erf}(L_b \sqrt{\beta})}, \quad (2-14)$$

where $\Delta_i = \delta_i / b$ is the normalized bond separation, $L_b = l_b / b$ is the normalized bond rest length, and

$$\beta = \frac{k_{LR} b^2}{2k_B T}. \quad (2-15)$$

In the bond rebinding rate equation, γ is a rebinding factor defined as

$$\gamma = \frac{k_{\text{on}}^0 l_{\text{bind}}}{k_0 b}, \quad (2-16)$$

which is a measure of propensity for rebinding to occur. Once the separation length δ has reached a value of roughly $2l_b$, rebinding of the ligand/receptor becomes almost impossible no matter how great the rebinding factor is [Qian et al. 2008].

In our model we consider both stochastic rebinding and rupturing of all bonds within a focal adhesion. The binding evolution of the bond cluster is characterized by the master equation [van Kampen 1992]

$$\frac{dP_n(\tau)}{d\tau} = \hat{g}_{n-1} P_{n-1}(\tau) + \hat{r}_{n+1}(\tau) P_{n+1}(\tau) - [\hat{r}_n(\tau) + \hat{g}_n(\tau)] P_n(\tau), \quad (2-17)$$

where $\tau = k_0 t$ is normalized time, n is the number of closed bonds in the adhesion, \hat{r}_n and \hat{g}_n correspond to the normalized total bond cluster rupture and rebinding rates when n bonds are closed (these rates differ from r_i and g_i which are rupture and rebinding rates for a single bond i), and $P_n(\tau)$ is the probability that n bonds are closed at time τ . Using a Monte Carlo method, which will be discussed in the next section, our model initially starts with n equal to the total number of bonds N within the focal adhesion. As time passes, stochastic binding and breaking occur until n equals zero, corresponding to failure of the adhesion as all the bonds within the focal adhesion become open.

3. Numerical method

To analyze (2-17) we use a Monte Carlo method based on Gillespie's algorithm [1976; 1977]. Initially all bonds within the focal adhesion are assumed to be closed. The evolution of the adhesion is characterized

total number of bonds, N	6–90
spacing between neighboring bonds, b	32 nm
focal adhesion size, $2a$	$\sim 0.2\text{--}3\ \mu\text{m}$
bond rest length, l_b	11 nm
radius of bond, a_0	5 nm
single bond stiffness, k_{LR}	0.25 pN/nm
combined elastic modulus, E^*	2–400 kPa
rebinding rate factor, γ	100
load factor, φ	0.44–0.52
force scale in bond dissociation, F_b	4 pN
shape factor, S	0–2
Boltzmann's constant \times temperature, $k_B T$	4.1 pN·nm

Table 1. Parameters used in the model of a focal adhesion between a cell and a substrate.

by cycles in which bond rupturing or rebinding occurs. Whether a closed bond will rupture or an open bond will rebind is determined by the probability of these actions occurring. The idea is to determine using randomized numbers and probability the likely location of a particular bond rupturing or rebinding for each cycle during the focal adhesion's lifetime until every bond in the focal adhesion is open. The likelihood of bond rupture/rebinding to occur at a specific location becomes dependent on the elastic solutions of the model at that current cycle time, and is globally based on the parameters used to define the specific focal adhesion under study, which are listed for our model in Table 1. It is necessary to note that because of the stochastic behaviors of both bond rupturing and rebinding for the focal adhesion, many simulations of each particular parameter set of focal adhesion must be performed and their output results averaged in order to formulate a reasonable assessment representative of the behavior of the adhesion.

In the present study, we analyze our model using the “first reaction method” of Gillespie's algorithm, following [Erdmann and Schwarz 2004a; 2004b]. In the first reaction method, a series of independent numbers are randomly generated in which they are uniformly distributed from 0 to 1. Each random number ξ_i is assigned to a specific bond site such that $\xi = (\xi_1, \dots, \xi_N)$ where N is the total number of bonds in the focal adhesion. The normalized reaction time for each specific bond site is calculated as [Gillespie 1976; 1977].

$$d\tau_i = -\frac{\ln \xi_i}{q_i}, \quad (3-1)$$

where q_i is either the normalized rebinding rate if the bond classified by index i is open or the normalized rupture rate if the bond is closed. The normalized reaction time for the particular cycle is chosen to be the minimum component of $d\tau_i$ such that,

$$d\tau = \min(d\tau_i), \quad (3-2)$$

where the location of actual reaction taking place is identified as where the shortest reaction time is chosen. This means that if the chosen bond at the reaction location is currently closed, the bond will rupture, and if the chosen bond is currently open, it will rebind, and the normalized time between the

reaction just prior to this one and the reaction just after this one is $d\tau$. Each time this reaction occurs constitutes one cycle and the number of cycles continues to grow until all bonds in the focal adhesion are open, which we have defined as the point when adhesion fails. The normalized lifetime of the focal adhesion is defined as the sum of all the reaction times for each cycle,

$$\tau = \sum_{k=1}^{\mu} d\tau_k, \quad (3-3)$$

where μ is the total number of cycles leading up to adhesion failure. This process is repeated a prescribed number of times and a normalized mean lifetime is determined.

4. Results

The first class of focal adhesions we chose to model were three types of focal adhesions with varying combined elastic modulus E^* values of 200 kPa, 100 kPa, and 20 kPa. For the model we chose a rebinding factor $\gamma = 100$ which is representative of highly favorable rebinding conditions [Qian et al. 2008; 2009], and a load factor $\varphi = 0.46$ which corresponds to the applied tensile load on the system being $\rho = 1.78$ kPa where $\rho = F/2ab$ and $F = \varphi F_b N$. The model is defined to represent a focal adhesion being experimented on at room temperature, corresponding to a value of $k_B T = 4.1$ pN · nm. Each ligand/receptor bond of the adhesion was modeled as a Hookean spring with a spring coefficient of $k_{LR} = 0.25$ pN/nm, which has been estimated as an appropriate value when modeling fibronectin/integrin bonds [Erdmann and Schwarz 2006]. The force factor defined for bond rupturing was chosen to be a constant value $F_b = 4$ pN [Erdmann and Schwarz 2004a; 2004b]. The ligand/receptor dimensions were defined to have a rest length $l_b = 11$ nm [Zuckerman and Bruinsma 1998] and an individual radius of $a_0 = 5$ nm [Arnold et al. 2004]. Each ligand/receptor bond is evenly spaced a distance $b = 32$ nm from each other, with the length of the entire focal adhesion defined as $2a$ and the total number of bonds in the adhesion as $N = 2a/b$. As shown in the left column of Figure 3, for each value of E^* , we varied the number of bonds making up the focal adhesion from 6 to 90, and for each focal adhesion size we varied the shape factor S within $[0, 2]$ in order to analyze each focal adhesion's mean lifetime. This range in number of bonds corresponds to a focal adhesion size of roughly 200 nm - 3 μ m.

Figure 3, top left, shows a clear increase in adhesion lifetime as the contact surface shape progresses towards the optimal shape, especially as the focal adhesion increases in size. However, as the adhesion increases in size, the optimal shape remains to have the maximum adhesion lifetime, but any discrepancies from this optimal shape result in a much lower adhesion lifetime. This is most clearly seen in Figure 3, top right, in which the adhesion lifetime is plotted against the number of bonds for shape factor values $S = 0, 0.8, 1$. The optimal shape represented in the graph by $S = 1$ clearly has the longest adhesion lifetime. However, as the adhesion grows in size, subtle variance from the optimal surface shape results in a drastic change in adhesion lifetime, which can be seen by comparing the lifetimes of $S = 0.8$ and $S = 1$. The difference between the two focal adhesion shapes is geometrically subtle, but the effect it has on adhesion lifetime becomes very drastic as the focal adhesion grows in size. These shape effects have also been studied in other areas of biology with regards to gecko adhesion, and similar results pertaining to adhesion strength were seen [Gao and Yao 2004]. A significant difference in adhesion lifetime appears to occur once the focal adhesion expands to 50 bonds when comparing the two surface shapes. This

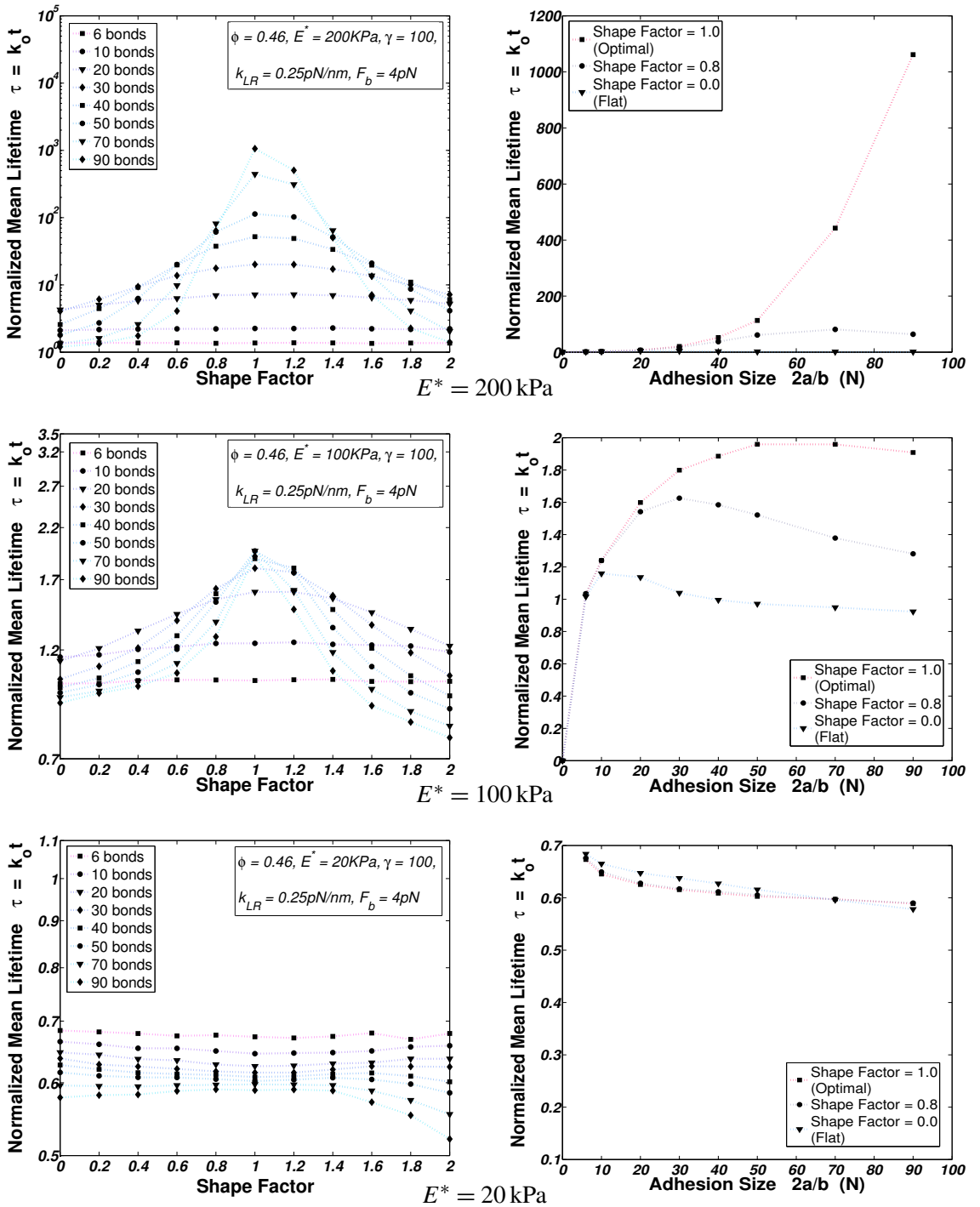


Figure 3. Effects of varying surface shape as defined by numerical shape factor values ranging within [0,2] on focal adhesion lifetime for different focal adhesion sizes ranging from 6 to 90 individual bonds. From top to bottom, $E^* = 200 \text{ kPa}, 100 \text{ kPa}, 20 \text{ kPa}$.

difference in lifetime increases more drastically as the adhesion continues to grow in size. This drastic reduction in adhesion lifetime for larger bonds with varying adhesion surface geometry from the optimal shape can be understood by the fact that generally stress concentrations are more severe as the focal adhesion increases in size [Qian et al. 2008; 2009]. What the optimal shape does for adhesion lifetime is to remove the preexisting stress concentrations from the bond cluster at its initial state. Therefore, the optimal contact shape can improve the lifetime of a cluster of bonds more significantly in larger adhesions.

The next type of focal adhesion modeled can be seen in Figure 3, middle left, in which the number of bonds within the adhesion varies from 6 to 90, the shape factor's observed range in $[0, 2]$, and the combined elastic modulus $E^* = 100$ kPa. Comparing the focal adhesion lifetimes between $E^* = 200$ kPa and $E^* = 100$ kPa shows that the adhesion lifetimes are much smaller for the softer system. This is concurrent to the results shown in other studies of system stiffness and adhesion lifetime [Qian et al. 2008; 2009]. Besides this difference in magnitude of adhesion lifetime, the behavior of the data in the case of $E^* = 100$ kPa seems to differ when compared to the results shown in Figure 3, top left. The focal adhesion still has the longest lifetime on the optimal contact surface shape, but the largest focal adhesion size does not correspond to the longest adhesion lifetime. This is more clearly seen in Figure 3, middle right, where the maximum adhesion lifetime is achieved for the optimal shape $S = 1$, when the adhesion contains about 50 bonds. After this critical size, the lifetime of the focal adhesion appears to shorten as the number of bonds increases. Similar behavior occurs for $S = 0.8$ where the critical number of bonds is 30, and for the flat surface $S = 0$ where the critical number of bonds is 10. A possible reason for this behavior, which has been previously studied for flat surface adhesion [Qian et al. 2008; 2009] is that as focal adhesions increase in size, they develop large stress concentrations at edges of the focal adhesion, and these stress concentrations result in crack-like failure of the focal adhesion, thereby decreasing its lifetime. Since the optimal shape was defined as the cell surface shape which results in the initially even distribution of load among all closed bonds, as the focal adhesion continues to cycle in which bonds are rupturing and rebinding, we believe that crack-like singularities begin to form within the adhesion domain and eventually dominate adhesion lifetime. This behavior of decreased adhesion lifetime with increasing adhesion size is also seen in the top row of Figure 3 for $E^* = 200$ kPa for the majority of nonoptimal cases, and we believe if the adhesion size continues to increase in bond number this behavior would then be seen even in the optimal case, as has been displayed for $E^* = 100$ kPa.

The bottom row of Figure 3 shows the results for a focal adhesion with combined elastic modulus $E^* = 20$ kPa. The data acquired for this focal adhesion differs greatly in comparison to the $E^* = 200$ kPa, 100 kPa cases mainly because the longest adhesion lifetimes seem to occur when the adhesion is very small. Also, the longest adhesion lifetime for most of the adhesion sizes seems to occur when the geometry of the adhesive surface is flat. Not until the adhesion reaches a size of roughly 70 bonds does the behavior of the focal adhesion lifetime seem to resemble that of the behavior shown in the above two cases. However, even in the case of optimal shape involving 90 bonds where the adhesion lifetime is longest, it still is shorter when compared to the adhesion lifetimes for any adhesion size and shape factor analyzed. From this data it appears that once the system reaches a critical stiffness threshold between soft matter and very soft matter, the effects of bond size on the adhesion outweigh the potential strengthening effects of shape on the adhesion. It also appears that optimizing the shape seems to decrease adhesion lifetime slightly, which differs in behavior from the previous two cases. However, the reasoning for these

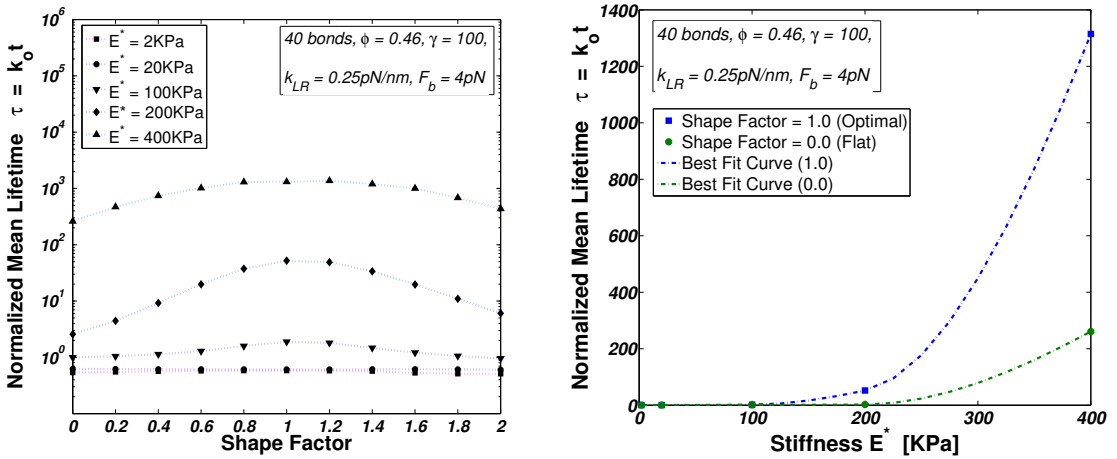


Figure 4. The effects of varying system stiffness as defined by the combined elastic modulus E^* on focal adhesion lifetime for an adhesion made up of 40 bonds with a load factor of $\phi = 0.46$. Left: focal adhesion lifetime as a function of the surface shape factor for values of $E^* = 2, 20, 100, 200, 400$ kPa. Right: focal adhesion lifetime as a function of system stiffness for the flat surface case ($S = 0$) and the optimal surface case ($S = 1$).

unexpected results could be because the load applied to the adhesion defined by a load factor of $\phi = 0.46$ is too great. The range in mean normalized lifetimes of all the adhesion sizes for the $E^* = 20$ kPa case only extends a normalized time frame of 0.1 which, when compared to the cases of $E^* = 100$ kPa and 200 kPa, is roughly 10 and 10,000 times smaller. In order to get a more thorough analysis of the effects of shape on a system of very soft stiffness, the load factor would have to be reduced in such a way that from the data shown here, a normalized time range of at least 1 would have to be represented. This would allow for a better representation of the effects of shape on adhesion systems with very soft cell and substrate.

For further understanding on the effects of contact surface shape on adhesion lifetime, an adhesion made up of 40 bonds was analyzed under varying stiffness values and varying load factor values. In Figure 4, a 40-bond focal adhesion was analyzed with a load factor of $\phi = 0.46$, a rebinding factor of $\gamma = 100$, and the combined elastic stiffness of the system ranged $E^* = 2$ kPa, 20 kPa, 100 kPa, 200 kPa, 400 kPa. From the left part of the figure, we see that the adhesion with optimal surface shape has the longest adhesion lifetime for the cases of $E^* = 100$ kPa and greater, and it appears that the adhesion lifetime gets exponentially longer as the stiffness of the system doubles in magnitude. Also as expected, due to the medium focal adhesion size, the difference between slight deviations from the optimal shape does not seem to have the drastic effect it had for larger bond sizes. However, it can be seen in Figure 4, right, that there is a large difference between adhesion lifetime between the optimal surface shape and the flat surface shape. This difference is large enough such that any attempt of optimizing the shape of the adhesion would have a substantial increase in the lengthening of adhesion lifetime, especially in cases where the system stiffness is large.

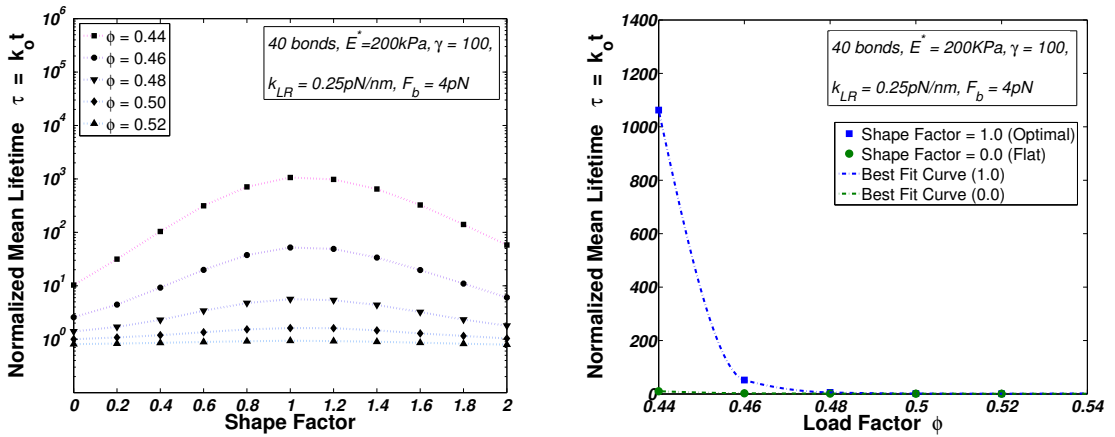


Figure 5. The effects of varying applied tensile load acting on the cell/substrate as defined by the load factor ϕ on focal adhesion lifetime for an adhesion made up of 40 bonds with a combined elastic modulus of $E^* = 200$ kPa. Left: focal adhesion lifetime as a function of the surface shape factor for values of $\phi = 0.52, 0.50, 0.48, 0.46, 0.44$. Right: focal adhesion lifetime as a function of the applied load for the flat surface case ($S = 0$) and the optimal surface case ($S = 1$).

In [Figure 5](#), a similar 40-bond focal adhesion is considered with a combined elastic modulus of $E^* = 200$ kPa, a rebinding factor of $\gamma = 100$, and the load factor for the adhesion is varied such that $\phi = 0.52, 0.50, 0.48, 0.46, 0.44$. As with the previous model involving varying system stiffness, the focal adhesion with the optimal surface shape has the longest adhesion lifetime and the difference in lifetime appears to increase exponentially as the load decreases, which is to be expected. The effects the shape of the adhesion surface has on adhesion lifetime seem to be more substantially affected by decreasing the load factor than varying the stiffness, which is shown by the greater normalized lifetime difference between the optimal and flat surface cases displayed in [Figure 5](#), right. However there appears to be substantially more sensitivity to deviations from the optimal shape as the load decreases in magnitude in comparison to the effects of deviation from the optimal shape for the increasing stiffness case. This can be taken to mean that decreasing the applied tensile load on an adhesion of large size with some geometrical variance from the optimal shape would be less effective in increasing the focal adhesion lifetime than would be done by increasing the system stiffness.

5. Conclusion

In this paper we have examined an idealized model of a cell/substrate focal adhesion bonded together by ligand/receptor bonds evenly spaced along curved surfaces. The focal adhesion was modeled as a bond cluster between continuous elastic media undergoing an applied tensile load which is distributed as traction forces on each bond. Initially all bonds in the adhesion were considered to be closed and the magnitude of the distributed traction forces on individual bonds was determined by the geometrical shape of the contact surface. The contact surface shape was defined by a numeric shape factor S in proportion to

an optimal shape that renders the applied tensile load being uniformly distributed among all closed bonds whenever these bonds are evenly spaced within the adhesion domain. The model accounted for both bond rupturing and rebinding via stochastic equations, which were analyzed numerically using Monte Carlo methods. A series of simulations were performed using a coupling of elastic and stochastic equations in order to model several sets of focal adhesions in which the effects of contact surface shape were observed with respect to the adhesion lifetime. In our model we have chosen to define adhesion lifetime as the time taken for all bonds within the adhesion to go from their initial state to failure. The calculated adhesion lifetimes were normalized using k_0 , the spontaneous dissociation rate of an individual bond in the absence of any type of load. The following main conclusions can be drawn from our analysis.

- (1) As the contact surface shape begins to change from flat towards the optimal shape for adhesion, the lifetime of the focal adhesion increases to a maximum value. The optimal surface shape is defined to have a shape factor of $S = 1$. Depending on the size of the focal adhesion and the number of ligand/receptor bonds within the adhesion, the advantage of having an optimal surface shape in increasing adhesion lifetime becomes more significant as the adhesion increases in size.
- (2) The larger the adhesion size becomes, the more drastic the effect slight deviations from the optimal contact surface shape have on the focal adhesion lifetime. Similar behavior has been demonstrated for adhesion of elastic media via van der Waals forces [Gao and Yao 2004; Yao and Gao 2006], as well as vesicles adhering on curved substrates [Shi et al. 2006].
- (3) As the size of a focal adhesion increases, the effect of the increased adhesion lifetime due to optimal surface shape begins to be overtaken by crack-like singularity behaviors which result in earlier failure of the focal adhesion. This transition of adhesion behavior leads to the observation of a critical adhesion size that corresponds to a maximum adhesion lifetime for the prescribed focal adhesion parameters. Even though the optimal surface shape almost always corresponds to the maximum adhesion lifetime (except in the case of very soft matter), as the focal adhesion increases in size, the adhesion lifetime begins to decrease after extending past a critical focal adhesion size. This is consistent with the behavior that occurs with flat surface focal adhesion as it increases in size [Qian et al. 2008; 2009].
- (4) In comparing the cases of increasing system stiffness or decreasing the magnitude of the applied tensile load in order to increase focal adhesion lifetime, it seems that both cases amplify the effects of optimal shape by a greater magnitude in comparison to the nonoptimized flat adhesion surface orientation. However, decreasing the applied load seems to be less effective in mitigating the effects of reduced adhesion lifetime due to deviations from the optimal surface shape in comparison to increasing system stiffness for a single focal adhesion. It is worthwhile to note that the sensitivity of focal adhesions to cell/substrate stiffness cannot be alleviated by removing stress concentration through optimal shape design. Even for molecular clusters under initially uniform pulling forces, the cell/substrate elasticity can destabilize focal adhesions by suppressing rebinding of open bonds [Qian and Gao 2010].

Experiments have shown that nanostructured surfaces have great impacts on cellular behavior and tissue engineering. The concepts developed in this paper should be understood as a theoretical model displaying the effects of surface geometry on adhesion lifetime for molecular adhesion based on specific ligand/receptor bonds. The present study shows from Monte Carlo simulations of discrete bond evolution that the contact surface shape could greatly influence the stability of cell-matrix adhesion. The analysis

by Wang and Gao [2010] based on a continuum formulation of cell-substrate interaction led to similar shape-dependent adhesion. This principle of optimal adhesion shape has already been quantitatively demonstrated by experiments in the case of nonspecific adhesion [Waters et al. 2011] and is now being analyzed and studied for specific adhesion as well. Once proven, we could contemplate further controlled experiments to explore using the micro- and nanoscale surface geometry to probe cell-matrix interactions.

References

- [Alberts et al. 2002] B. Alberts, A. Johnson, J. Lewis, M. Raff, R. Keith, and P. Walter, *Molecular biology of the cell*, 4th ed., Garland Science, New York, 2002.
- [Arnold et al. 2004] M. Arnold, E. A. Cavalcanti-Adam, R. Glass, J. Blümmel, W. Eck, M. Kantelehner, H. Kessler, and J. P. Spatz, “Activation of integrin function by nanopatterned adhesive interfaces”, *ChemPhysChem* **5**:3 (2004), 383–388.
- [Bell 1978] G. I. Bell, “Models for the specific adhesion of cells to cells”, *Science* **200**:4342 (1978), 618–627.
- [Bershadsky et al. 2003] A. D. Bershadsky, N. Q. Balaban, and B. Geiger, “Adhesion-dependent cell mechanosensitivity”, *Annu. Rev. Cell Dev. Biol.* **19** (2003), 677–695.
- [Chen and Gumbiner 2006] X. Chen and B. M. Gumbiner, “Crosstalk between different adhesion molecules”, *Curr. Opin. Cell Biol.* **18**:5 (2006), 572–578.
- [Erdmann and Schwarz 2004a] T. Erdmann and U. S. Schwarz, “Stability of adhesion clusters under constant force”, *Phys. Rev. Lett.* **92**:10 (2004), 108102.
- [Erdmann and Schwarz 2004b] T. Erdmann and U. S. Schwarz, “Stochastic dynamics of adhesion clusters under shared constant force and with rebinding”, *J. Chem. Phys.* **121**:18 (2004), 8997–9017.
- [Erdmann and Schwarz 2006] T. Erdmann and U. S. Schwarz, “Bistability of cell-matrix adhesions resulting from nonlinear receptor-ligand dynamics”, *Biophys. J.* **91**:6 (2006), L60–L62.
- [Erdmann and Schwarz 2007] T. Erdmann and U. S. Schwarz, “Impact of receptor-ligand distance on adhesion cluster stability”, *Eur. Phys. J. E* **22**:2 (2007), 123–137.
- [Evans 2001] E. A. Evans, “Probing the relation between force—lifetime—and chemistry in single molecular bonds”, *Annu. Rev. Biophys. Biomol. Struct.* **30** (2001), 105–128.
- [Evans and Calderwood 2007] E. A. Evans and D. A. Calderwood, “Forces and bond dynamics in cell adhesion”, *Science* **316**:5828 (2007), 1148–1153.
- [Evans and Ritchie 1997] E. A. Evans and K. Ritchie, “Dynamic strength of molecular adhesion bonds”, *Biophys. J.* **72**:4 (1997), 1541–1555.
- [Gao and Yao 2004] H. Gao and H. Yao, “Shape insensitive optimal adhesion of nanoscale fibrillar structures”, *Proc. Nat. Acad. Sci. USA* **101**:21 (2004), 7851–7856.
- [Gillespie 1976] D. T. Gillespie, “A general method for numerically simulating the stochastic time evolution of coupled chemical reactions”, *J. Comput. Phys.* **22**:4 (1976), 403–434.
- [Gillespie 1977] D. T. Gillespie, “Exact stochastic simulation of coupled chemical reactions”, *J. Phys. Chem.* **81**:25 (1977), 2340–2361.
- [Johnson 1985] K. L. Johnson (editor), *Contact mechanics*, Cambridge University Press, New York, 1985.
- [van Kampen 1992] N. G. van Kampen, *Stochastic processes in physics and chemistry*, North-Holland, New York, 1992.
- [Lo et al. 2000] C.-M. Lo, H.-B. Wang, M. Dembo, and Y.-L. Wang, “Cell movement is guided by the rigidity of the substrate”, *Biophys. J.* **79**:1 (2000), 144–152.
- [Pelham and Wang 1997] R. J. Pelham, Jr. and Y.-L. Wang, “Cell locomotion and focal adhesions are regulated by substrate flexibility”, *Proc. Nat. Acad. Sci. USA* **94**:25 (1997), 13661–13665.
- [Qian and Gao 2010] J. Qian and H. Gao, “Soft matrices suppress cooperative behaviors among receptor-ligand bonds in cell adhesion”, *PLoS ONE* **5**:8 (2010), e12342.

- [Qian et al. 2008] J. Qian, J. Wang, and H. Gao, “Lifetime and strength of adhesive molecular bond clusters between elastic media”, *Langmuir* **24**:4 (2008), 1262–1270.
- [Qian et al. 2009] J. Qian, J. Wang, Y. Lin, and H. Gao, “Lifetime and strength of periodic bond clusters between elastic media under inclined loading”, *Biophys. J.* **97**:9 (2009), 2438–2445.
- [Shi et al. 2006] W. Shi, X. Q. Feng, and H. Gao, “Two-dimensional model of vesicle adhesion on curved substrates”, *Acta Mech. Sinica* **22**:6 (2006), 529–535.
- [Tan et al. 2003] J. L. Tan, J. Tien, D. M. Pirone, D. S. Gray, K. Bhadriraju, and C. S. Chen, “Cells lying on a bed of microneedles: an approach to isolate mechanical force”, *Proc. Nat. Acad. Sci. USA* **100**:4 (2003), 1484–1489.
- [Wang and Gao 2010] J. Wang and H. Gao, “Size and shape dependent steady-state pull-off force in molecular adhesion between soft elastic materials”, *Int. J. Fract.* **166**:1–2 (2010), 13–19.
- [Waters et al. 2011] J. F. Waters, H. J. Gao, and P. R. Guduru, “On adhesion enhancement due to concave surface geometries”, *J. Adhes.* **87**:3 (2011), 194–213.
- [Yao and Gao 2006] H. Yao and H. Gao, “Optimal shapes for adhesive binding between two elastic bodies”, *J. Colloid Interface Sci.* **298**:2 (2006), 564–572.
- [Zaidel-Bar et al. 2003] R. Zaidel-Bar, C. Ballestrem, Z. Kam, and B. Geiger, “Early molecular events in the assembly of matrix adhesions at the leading edge of migrating cells”, *J. Cell Sci.* **116**:22 (2003), 4605–4613.
- [Zamir et al. 2000] E. Zamir, M. Katz, Y. Posen, N. Erez, K. M. Yamada, B.-Z. Katz, S. Lin, D. C. Lin, A. Bershadsky, Z. Kam, and B. Geiger, “Dynamics and segregation of cell-matrix adhesions in cultured fibroblasts”, *Nat. Cell Biol.* **2**:4 (2000), 191–196.
- [Zuckerman and Bruinsma 1998] D. M. Zuckerman and R. F. Bruinsma, “Vesicle-vesicle adhesion by mobile lock-and-key molecules: Debye–Hückel theory and Monte Carlo simulation”, *Phys. Rev. E* **57**:1 (1998), 964–977.

Received 1 Apr 2010. Revised 28 Sep 2010. Accepted 30 Sep 2010.

GREGORY J. RIZZA: gregory_rizza@brown.edu

Solid Mechanics Group, School of Engineering, Brown University, Providence, RI 02912, United States

JIN QIAN: jqian9@mail.gatech.edu

Coulter Department of Biomedical Engineering, Georgia Institute of Technology, Atlanta, GA 30332, United States

HUAJIAN GAO: hujian_gao@brown.edu

Solid Mechanics Group, School of Engineering, Brown University, Providence, RI 02912, United States